Evaluation of a Numerical Method for Identifying Surface Acoustic Impedances in a Reverberant Room

Niccolò Antonello, Toon van Waterschoot[a], Marc Moonen
KU Leuven, Dept. of Electrical Engineering (ESAT), STADIUS Center for Dynamical Systems, Signal Processing and Data Analytics, Kasteelpark Arenberg 10, 3001 Leuven, Belgium

Patrick A. Naylor
Imperial College London, Dept. of Electrical Engineering, SW7 2AZ, London, United Kingdom

Summary

Wave-based room acoustic simulations are becoming more popular as the available compute power continues to increase. The definition of boundary conditions and acoustic impedances is of fundamental importance for these simulations to succeed in representing a realistic acoustical space. Acoustic impedance databases exist in terms of absorption coefficients, which are usually measured in reverberation chambers. In this type of measurements, the sound field is assumed to be diffuse, a condition which is not met in most rooms. In particular at low frequencies, where wave-based simulations are possible, a different approach is sought as an alternative to acoustic impedance measurements. This paper focuses on a recently proposed method for estimating surface acoustic impedances. This method is based on the use of a numerical room model, and does not require the assumption of a diffuse field. Assuming that the geometry of the room is known, a finite difference time domain (FDTD) simulation is matched with measured data by solving an optimization problem. The set-up for such a measurement method consists only of a set of microphones and a loudspeaker. This could be applied in every room, removing the need for expensive facilities such as reverberation chambers. The solution of the optimization problem leads to the sought parameters of the acoustic surface impedances. In this paper the adjoint method is used for the computation of the derivative in the optimization problem. This method enables a large number of decision variables in the optimization problem making it possible to account for inhomogeneities of the surface acoustic impedance and hence to avoid the need to specify the different acoustic impedance surfaces beforehand.

PACS no. 43.60.+d, 43.58.+z

[a]also affiliated with Dept. of Electrical Engineering (ESAT), ETC, AdvISe Lab, Kleinhoefstraat, 2440 Geel, Belgium

1. Introduction

Wave-based room acoustic simulations are becoming more popular as the available compute power continues to increase. In particular, the finite difference time domain (FDTD) method is receiving a lot of attention especially since its boundary model formulation was improved [1]. However, there is a lack of input parameters for this boundary model, i.e. of measured acoustic impedances. In fact acoustic impedances are usually measured in terms of absorption coefficients using reverberation chambers where the sound field is assumed to be diffuse [2]. Such an ideal sound field rarely occurs in real rooms and is indeed also not present in low frequency wave-based simulations. Therefore the usage of these absorption coefficients as input parameters for wave-based simulations is questionable.

In [3] a new method for estimating acoustic impedances was proposed. Assuming the room geometry and source distribution to be known, an optimization problem that minimizes the misfit between simulated and measured sound pressure was solved to obtain an estimation of the acoustic impedances. Using the boundary element method (BEM) for the wave-based room acoustic simulation, the optimization problem was posed for singular frequencies, therefore requiring extensive spatial sampling. An alternative approach using the FDTD method was presented in [4] where it was shown that the setup can be greatly simplified and reduced to a loudspeaker and a set of microphones when a narrowband simulation is performed.

In this paper the optimization algorithm of [4] is further developed. Here, the adjoint method is used, which enables the efficient computation of the gradient of the cost function almost independently of the number of the decision variables of the optimization problem. In [3,4] each acoustic impedance surface, e.g. each wall of the room, was modeled using a single acoustic impedance. It is shown here that if inhomogeneities are present in the acoustic impedance surfaces this can lead to a failure of the method. Using the adjoint method it is possible to seek for a different acoustic impedance at each point of the discretized boundary surfaces. Therefore, if inhomogeneities are present, these will be reconstructed. Moreover there is no longer a need to specify the acoustic impedance surfaces manually. Having an increased number of decision variables, however, the main disadvantage of the presented method is that the optimization problem can become ill-posed for certain measured data sets and a regularization is necessary. The adjoint method has been widely used in other fields such as full-waveform inversions in geophysics [5] and imaging techniques [6] but its application for acoustic impedance identification in room acoustic has so far not been studied, to the best of authors' knowledge.

2. The finite difference time domain method

The sound field in a room may be predicted by solving the acoustic wave equation, e.g. using the following partial differential equation (PDE), boundary conditions (BCs) and initial conditions (ICs) [2]:

$$\begin{aligned} &\text{PDE} \quad \triangle p - \frac{1}{c^2}\frac{\partial^2 p}{\partial t^2} = s \text{ on } \Omega \times \tau \\ &\text{BCs} \quad \frac{\partial p}{\partial t} = -c\xi \nabla p \cdot \mathbf{n} \text{ on } \partial\Omega \times \tau \\ &\text{ICs} \quad \frac{\partial p}{\partial t} = \hat{p}_0, p = p_0 \text{ on } \Omega \end{aligned} \tag{1}$$

where $\Omega \subset \mathbb{R}^3$ is the spatial domain defining the room geometry, $\tau \subset \mathbb{R}^+$ is temporal domain, $p(x,y,z,t) : \mathbb{R}^4 \to \mathbb{R}$ is the sound pressure, $s(x,y,z,t)$ is the source distribution, $\triangle$ is the Laplacian operator, $\mathbf{n}$ is the normal vector with respect to the boundary surface $\partial\Omega$, $\xi : \partial\Omega \to \mathbb{R}$ is the specific acoustic impedance , c is the speed of sound and $\hat{p}_0$, $p_0 : \mathbb{R}^3 \to \mathbb{R}$ are the ICs.

Analytical solutions of (1) exist only for simple geometries and hence it is typically necessary to perform a discretization. The FDTD method discretizes the sound pressure and source distribution in a uniform grid with spatial resolution X, and in time with temporal resolution T, e.g. for the sound pressure

$$p(x,y,z,t) \approx p(lX, mX, iX, nT) = p^n_{l,m,i}. \tag{2}$$

Centered finite differences are applied to approximate the second-order derivatives of (1). Spatial and temporal resolution are bounded for stability reasons by the ratio $\frac{cT}{X} \leq \lambda_c$, where λ_c is the Courant number, i.e. the maximum ratio between spatial and temporal resolution where stability is ensured and numerical errors are minimized [1]. When explicit FDTD schemes are employed this approximation leads to the update equation

$$p^{n+1}_{l,m,i} = P^n_{l,m,i} - p^{n-1}_{l,m,i} + s^n_{l,m,i}, \tag{3}$$

which represent the PDE of (1). The term $P^n_{l,m,i}$ represents the approximation of the Laplacian which consists of the weighted sum of the 26 neighbor samples of $p^n_{l,m,i}$ and $p^n_{l,m,i}$ itself. Different weight choices lead to different FDTD schemes which can be found in [1]. In this paper the 19-samples ISO1 scheme will be employed.

When at the boundary, $P^n_{l,m,i}$ will miss a number of neighbor samples, depending on the nature of the boundary, e.g. walls, inner/outer edges, inner/outer corners and other cases. These missing neighbor samples can be used to enforce the BCs of (1) as well as continuity conditions. The modified update equation will become, e.g. for a wall:

$$(1 + \lambda_c/\xi_b)\, p^{n+1}_{l,m,i} = \tilde{P}^n_{l,m,i} + (\lambda_c/\xi_b - 1)\, p^{n-1}_{l,m,i}, \tag{4}$$

where $\tilde{P}^n_{l,m,i}$ is the weighted sum having 9 neighbor samples missing and modified weights due to enforced BCs. Notice that the subscript index b indicates the position of ξ_b on the discretization of $\partial\Omega$.

Problem (1) is converted into a set of linear equations that is typically solved iteratively using equations (3), (4) and other equations obtained from other types of BCs. Nevertheless, for illustration purposes, it is convenient to look at the structure of the matrices that arise in such a linear system. By vectorizing the tensors $p^n_{l,m,i}$ and $s^n_{l,m,i}$ for each n, it is possible to group all the equations and write:

$$\mathbf{Q}_+ \mathbf{p}_{n+1} - \mathbf{A}\mathbf{p}_n - \mathbf{Q}_- \mathbf{p}_{n-1} = \mathbf{s}_n \tag{5}$$

where $\mathbf{Q}_+$ and $\mathbf{Q}_-$ are $N_x N_y N_z \times N_x N_y N_z$ diagonal matrices having ones at the indexes where the update equation is (3) and having coefficients e.g. $(1 + \lambda_c/\xi_b)$ and $(1 - \lambda_c/\xi_b)$ for the wall-modified update equation (4), respectively. The vectors $\mathbf{p}_n$ and $\mathbf{s}_n$ are $N_x N_y N_z$ dimensional vectors containing the vectorization of the sampled sound pressure $p^n_{l,m,i}$ and source distribution $s^n_{l,m,i}$ for the time samples n. Here N_x, N_y, N_z are the number of spatial samples used for each cardinal direction. The $\mathbf{A}$ matrix represents the approximation of the Laplacian and consists of a $N_x N_y N_z \times N_x N_y N_z$ sparse matrix having, for the general explicit scheme, 27 diagonals containing zero elements at the indexes where the BCs are enforced. Notice that the acoustic impedance ξ_b appears only in the matrices $\mathbf{Q}_\pm$.

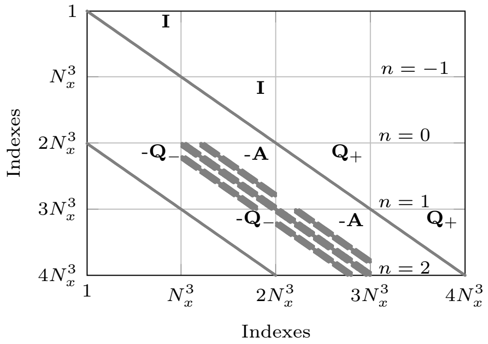

Figure 1. Sparsity pattern of the $\mathbf{B}$ matrix.

The final linear system of equations can be obtained by stacking all $\mathbf{p}_n$ and $\mathbf{s}_n$ into two compound vectors and is given as

$$\mathbf{B}\mathbf{p} = \mathbf{s}, \tag{6}$$

where $\mathbf{p}$ and $\mathbf{s}$ are now $N_x N_y N_z (N_t + 2)$ dimensional vectors. The sparsity pattern of $\mathbf{B}$ is shown in Fig. 1 for a cubic room having $N_x N_y N_z = N_x^3$ spatial samples and $N_t = 2$ temporal samples. It can be noticed that for $n = -1$ and $n = 0$ the ICs (here assumed to be zero) are enforced using an identity matrix $\mathbf{I}$.

3. The optimization algorithm

For a given room geometry and the source distribution, K microphones are used to record the sound field in the room for N_t time samples. The impedance vector $\boldsymbol{\xi} \in \mathbb{R}^{N_\xi}$, which contains N_ξ elements that model the acoustic impedance surfaces of the room, can be estimated by solving the following optimization problem [4]

$$\begin{aligned} \min_{\boldsymbol{\xi}} \quad & f = \frac{1}{2}\|\mathbf{F}\mathbf{p} - \tilde{\mathbf{p}}\|_2^2 \\ \text{s. t.} \quad & \mathbf{B}\mathbf{p} = \mathbf{s}, \\ & \boldsymbol{\xi}_{\min} \le \boldsymbol{\xi} \le \boldsymbol{\xi}_{\max}, \end{aligned} \tag{7}$$

The cost function f represents the misfit function, i.e. the l_2-norm of the residual between the measured sound pressure $\tilde{\mathbf{p}}$ and the sound pressure produced by the FDTD method at the microphone positions. $\mathbf{F}$ is a selection matrix that selects the KN_t samples out of $\mathbf{p}$ that correspond to the measured sound pressure samples of $\tilde{\mathbf{p}}$. The equality constraint is the linear system of equations given by the FDTD method and the inequalities are box constraints to prevent $\boldsymbol{\xi}$ to reach non-physical values e.g. a negative acoustic impedance.

Due to the fact that the acoustic impedances contained in $\boldsymbol{\xi}$ appear in the matrix $\mathbf{B}$, the equality constraint of (7) is nonlinear. This optimization problem is therefore non-convex and can be solved using sequential quadratic programming (SQP) [7]. Starting from an initial guess $\boldsymbol{\xi}_0$, and substituting the equality constraint into the cost function, (7) can be locally approximated by the following quadratic optimization problem:

$$\begin{aligned} \min_{\mathbf{p}_k} \quad & f(\boldsymbol{\xi}_k) + \nabla f(\boldsymbol{\xi}_k)^T \mathbf{d}_k + \mathbf{d}_k^T \nabla^2 f(\boldsymbol{\xi}_k) \mathbf{d}_k \\ \text{s. t.} \quad & \boldsymbol{\xi}_{\min} \le \boldsymbol{\xi} \le \boldsymbol{\xi}_{\max}, \end{aligned} \tag{8}$$

where the step $\mathbf{d}_k = \boldsymbol{\xi}_k - \boldsymbol{\xi}_{k-1}$ gives a new value $\boldsymbol{\xi}_k$. After having ensured with a proper line-search method [7] that the step gives a sufficient decrease of the cost function this procedure can be repeated iteratively until a local minimum is found.

At each iteration of the SQP method, the gradient $\nabla f(\boldsymbol{\xi}_k)$ and the Hessian $\nabla^2 f(\boldsymbol{\xi}_k)$ are needed. Typically $\nabla f(\boldsymbol{\xi}_k)$ is computed numerically, e.g. using finite difference, while the Hessian $\nabla^2 f(\boldsymbol{\xi}_k)$ is usually replaced by an approximation using techniques such as Gauss-Newton (GN) or BFGS [7], since its numerical computation is expensive. In [4] $\nabla f(\boldsymbol{\xi}_k)$ was evaluated using finite difference, which required the computation of a FDTD simulation for each component of $\boldsymbol{\xi}$. However, when the number of sought acoustic impedances is high, such an approach can easily become unfeasible. In the following subsection the adjoint method is described specifically for the FDTD approach. This method enables the calculation of the gradient with the computation of only two FDTD simulations, almost independently of the number of impedances [5].

3.1. The Adjoint Method

The derivative of the cost function with respect to an arbitrary acoustic impedance ξ_b may be written as

$$\frac{\partial f}{\partial \xi_b}(\boldsymbol{\xi}) = \frac{\partial \mathbf{p}}{\partial \xi_b}^T \mathbf{F}^T (\mathbf{F}\mathbf{p} - \tilde{\mathbf{p}}). \tag{9}$$

Here $\frac{\partial \mathbf{p}}{\partial \xi_b}$ represents the computational bottleneck for the computation of the gradient. Taking the derivative with respect to ξ_b of the equality constraint of (7)

$$\frac{\partial \mathbf{B}}{\partial \xi_b}\mathbf{p} + \mathbf{B}\frac{\partial \mathbf{p}}{\partial \xi_b} = 0, \tag{10}$$

it can be seen that $\frac{\partial \mathbf{B}}{\partial \xi_b}$ actually represents an extremely sparse matrix: looking at Fig. 1, ξ_b appears only in the diagonal matrices $\mathbf{Q}_\pm$ where the BCs are imposed. From (10) it follows that

$$\frac{\partial \mathbf{p}}{\partial \xi_b} = -\mathbf{B}^{-1}\frac{\partial \mathbf{B}}{\partial \xi_b}\mathbf{p} \tag{11}$$

and substituting this into (9), leads to

$$\frac{\partial f}{\partial \xi_b}(\boldsymbol{\xi}) = -\left[\frac{\partial \mathbf{B}}{\partial \xi_b}\mathbf{p}\right]^T \underbrace{\left[\mathbf{B}^{-1}\right]^T \mathbf{F}^T (\mathbf{F}\mathbf{p} - \tilde{\mathbf{p}})}_{\boldsymbol{\lambda}}, \tag{12}$$

where $\boldsymbol{\lambda}$ is the solution of the adjoint problem:

$$\boldsymbol{\lambda}^T \mathbf{B} = \mathbf{F}^T(\mathbf{F}\mathbf{p} - \tilde{\mathbf{p}}) = \hat{\mathbf{s}}. \tag{13}$$

Here $\hat{\mathbf{s}}$ consists of a new source distribution. The residual $(\mathbf{F}\mathbf{p} - \tilde{\mathbf{p}})$ is expanded into a vector of the same size as $\mathbf{p}$ due to the transpose of the selection matrix $\mathbf{F}$. Hence in the adjoint problem the source distribution consists of point sources appearing at the microphone positions where a particular source signal is given as the residual between measured and simulated signals of the corresponding microphone. It can be noticed that such a problem could be solved iteratively using:

$$-\mathbf{Q}_- \boldsymbol{\lambda}_{n+1} - \mathbf{A}^T \boldsymbol{\lambda}_n + \mathbf{Q}_+ \boldsymbol{\lambda}_{n-1} = \hat{\mathbf{s}}_n. \tag{14}$$

However, if a time inversion is applied the system of equations becomes the same as the one in (5) with the only difference that $\mathbf{A}$ is transposed and that the source distribution consists of a set of sources positioned at the microphone positions and where the source signals are now the time-reversed residuals. Finally, looking back at equation (12), it can be seen that in order to obtain the full gradient $\nabla f(\boldsymbol{\xi})$, each of the sparse matrices $\frac{\partial \mathbf{B}}{\partial \xi_b}$ for $i = 1 \dots N_\xi$ must be multiplied by $\mathbf{p}$ and these products are then multiplied by the solution of the adjoint problem $\boldsymbol{\lambda}$. Hence only two FDTD simulations are needed to obtain $\mathbf{p}$ and $\boldsymbol{\lambda}$ for each iteration of the SQP procedure.

A more natural choice of the decision variables of the optimization problem would be the admittance, i.e. the inverse of the acoustic impedance, $\upsilon = 1/\xi$. In fact, in the computation of $\frac{\partial \mathbf{B}}{\partial \upsilon_b}\mathbf{p}$ the derivative of (4) with respect to υ_b will simply be $\lambda_c(p^{n+1}_{l,m,i} - p^{n-1}_{l,m,i})$. If the derivative is with respect to ξ_b is computed, the acoustic impedance ξ_b would still be present in the last expression. For this reason, in the following the impedances will be replaced by admittances and the decision variables $\boldsymbol{\xi}$ will be represented by $\boldsymbol{\upsilon}$, the vector containing the admittances used to model the admittance surfaces. Hence, for the calculation of $\mathbf{p}$, it is only necessary to save the sound pressure difference $\lambda_c(p^{n+1}_{l,m,i} - p^{n-1}_{l,m,i})$ at the boundary positions, which represents computing $\frac{\partial \mathbf{B}}{\partial \upsilon_b}\mathbf{p}$. This data can then be used in the iterative procedure of solving the adjoint problem, to directly compute the product $(\frac{\partial \mathbf{B}}{\partial \upsilon_b}\mathbf{p})^T\boldsymbol{\lambda}$ of (12). Therefore neither $\mathbf{p}$ nor $\boldsymbol{\lambda}$ have to be fully stored.

3.2. Tikhonov regularization

The optimization problem (7) is an inverse problem and depending on the measured sound pressure $\tilde{\mathbf{p}}$ it can become ill-posed. This condition can occur when the microphone signals contain redundant information or when the system is not fully excited, e.g. when a narrowband signal is used in the source distribution. In fact, at high frequencies the solution of the FDTD method is corrupted by numerical errors. In particular, the isotropic scheme used in this paper has a numerical relative error inferior to 2% up to $0.175 f_s$, where f_s is the sampling frequency. Therefore the data fitting should be performed below this frequency upper limit. Moreover it is well known that admittances are frequency-dependent, meaning that their estimation should be performed in narrow bands where they can be assumed to be frequency-independent. In order to compensate for the ill-posed nature of the problem, the cost function can be modified by adding a Tikhonov regularization [8]

$$\hat{f} = f + \frac{\lambda_x}{2}\left(\|\mathbf{W}_x\boldsymbol{\upsilon}\|_2^2 + \|\mathbf{W}_y\boldsymbol{\upsilon}\|_2^2 + \|\mathbf{W}_{xy}\boldsymbol{\upsilon}\|_2^2\right), \tag{15}$$

where f is the misfit function found in (7), $\hat{f}$ is the regularized cost function and $\mathbf{W}_i$ are weighting matrices that approximate the gradient $\nabla_i \boldsymbol{\upsilon}$ on the admittance surface over the directions $i = (x, y, xy)$ using finite difference operators. This type of regularization enforces smoothness on the estimated admittance surfaces by minimizing their gradient. The parameter λ_x weights this smoothing operation over the misfit function. If there is a lack of information in $\tilde{\mathbf{p}}$ the regularization gives higher preference to a smooth solution. The weight of the smoothing operator should be carefully chosen not to be stronger than the weight of the misfit function, otherwise the optimization would not fully exploit all the information contained in the measured data.

The gradient of the regularized cost function becomes

$$\nabla \hat{f}(\boldsymbol{\upsilon}) = \nabla f(\boldsymbol{\upsilon}) + \lambda_x\left(\mathbf{W}_x^T\mathbf{W}_x\boldsymbol{\upsilon} + \mathbf{W}_y^T\mathbf{W}_y\boldsymbol{\upsilon} + \mathbf{W}_{xy}^T\mathbf{W}_{xy}\boldsymbol{\upsilon}\right), \tag{16}$$

where $\nabla f(\boldsymbol{\upsilon})$ is obtained using the adjoint method. The $\mathbf{W}_i$ matrices can be constructed as follows. Let the vector $\boldsymbol{\upsilon}$ be the vectorization of the admittances of the various surfaces of the room, e.g. for a cubic room

$$\boldsymbol{\upsilon} = [\boldsymbol{\upsilon}_{lw}^T, \boldsymbol{\upsilon}_{rw}^T, \boldsymbol{\upsilon}_{fw}^T, \boldsymbol{\upsilon}_{rew}^T, \boldsymbol{\upsilon}_c^T, \boldsymbol{\upsilon}_f^T]^T, \tag{17}$$

where the subscripts indicate left wall, right wall, front wall, rear wall, ceiling and floor. Let $\boldsymbol{\upsilon}_{lw}$ be an $N_x N_y$ vectorization of an $N_x \times N_y$ admittance surface obtained by stacking the N_x long columns of the admittance surface. A one-dimensional finite difference matrix can be constructed

$$\mathbf{D}_{x,1D} = \begin{pmatrix} 1 & -1 & & \\ & \ddots & \ddots & \\ & & 1 & -1 \end{pmatrix} \in \mathbb{R}^{(N_x-1)\times N_x} \tag{18}$$

which can be used to obtain the gradient of an N_x long vector. Let $\mathbf{I}_{N_y}$ be the $N_y \times N_y$ identity matrix, if a two dimensional finite difference operator over the

x direction is wanted, this can be obtained by the following Kronecker product

$$\mathbf{D}_{x,2D} = \mathbf{I}_{N_y} \otimes \mathbf{D}_{x,1D}. \tag{19}$$

Similarly the y direction gradient and the transverse direction gradient can be obtained by $\mathbf{D}_{y,2D} = \mathbf{D}_{y,1D} \otimes \mathbf{I}_{N_x}$ and $\mathbf{D}_{xy,2D} = \mathbf{D}_{y,1D} \otimes \mathbf{D}_{x,1D}$, respectively. The final $\mathbf{W}_i$ is given by the block diagonal matrix of the various $\mathbf{D}_{i,2D}$ for all the different admittance surface vectors contained in (17).

4. Simulation Results

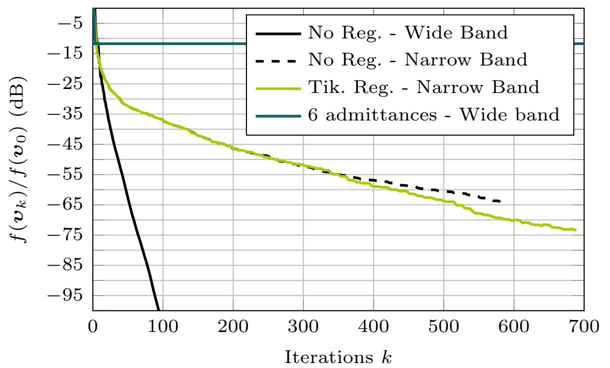

Figure 4. Convergence curve of the relative misfit function using wide band and narrow band source signals with no regularization, Tikhonov regularization using the adjoint method and using the method of [4].

The sound field of a cubic room of dimensions $4.4 \times 4.8 \times 5.3$ m^3 is first simulated using the FDTD method for 2 seconds, $N_t = 2f_s$. The sampling frequency is $f_s = 891$ Hz resulting in a spatially uniform grid of dimension $(N_x \times N_y \times N_z) = (10 \times 11 \times 12)$. Each wall has different admittance surfaces with inhomogeneities: these are shown in the top row of Fig. 2. A point source excites the system and 6 microphones at fixed random positions are used to obtain $\tilde{\mathbf{p}}$. This $\tilde{\mathbf{p}}$ is then used to invert the system and reconstruct the admittance surfaces as explained in section 3. The optimization procedure is stopped either when the reduction of the relative misfit function satisfies $f(\boldsymbol{\upsilon}_k)/f(\boldsymbol{\upsilon}_0) < \epsilon = 10^{-10}$, corresponding to -100 dB, or if line search failure occurs. The optimization problem is initialized for $\upsilon = 1/40$ for all values of $\boldsymbol{\upsilon}$. The sought $\boldsymbol{\upsilon}$ vector is a $2((N_x - 2 + N_y - 2)(N_z - 2) + (N_x - 2)(N_y - 2)) = 484$ dimensional vector. The -2 is due to the fact that the admittances parameters υ_b that appear at corners and edges are actually copied from the neighbor ones belonging to the admittance surfaces. This is done to enforce continuity between two or three intersecting admittance surfaces.

Fig. 3 shows the original $\boldsymbol{\upsilon}$ vector and the estimated one using the adjoint method described in section 3.1 (without regularization) and using the method presented in [4], where only 6 admittances are used to model each of the 6 admittance surfaces. The SQP is solved using damped BFGS for the adjoint method while GN [7] is used for the 6 admittances case. The source signal consists of wide band bandpass filtered white noise, between 20-440 Hz.

It can be noticed that when only 6 decision variables are used, the estimated admittances are good averages of the admittances of the corresponding admittance surfaces. However, as it can be seen in Fig. 4, the method fails to fit the data: the minimization is stopped due to line search failure after 10 iterations only and relative reduction of the misfit function reaches only -11 dB. On the other hand the adjoint method reaches the local minimum in 95 iterations and a perfect reconstruction is achieved, as can be seen in Fig. 3.

When a wideband signal is used, the optimization problem is well-posed and perfect reconstruction is achieved. This is not the case when a narrowband signal is used which, for the reasons described in section 3.2, would be the case when applying the method with real measured signals. In the following cases the source signal consists of bandpass filtered white noise between 44-88 Hz. If no regularization is applied, looking at the second row of Fig. 2, the estimated admittance surfaces resemble the original ones only partially. Moreover, in Fig. 4, it can be seen how the convergence rate of the SQP is reduced and a relative reduction of -64 dB is achieved. Nevertheless, using Tikhonov regularization, this situation can be slightly improved: after tuning the regularization parameter to $\lambda_x = 2 \cdot 10^{-3}$, it can be noticed how in Fig. 2 the estimated surfaces are indeed smoother and resemble much more the original ones. The convergence rate is also improved and the misfit reaches a relative reduction of -73 dB, as shown in Fig. 4.

5. Conclusions

The adjoint method was used to solve an optimization problem that can estimate the acoustic impedance surfaces. The room acoustics were modeled using the FDTD method. Compared to previous works [3,4], it has been shown that using only one decision variable to model each of the acoustic impedance surfaces can lead to the failure of the methods of [3, 4]. The adjoint method enables the usage of large numbers of decision variables so that the acoustic impedance surfaces can be accurately estimated even when inhomogeneities are present. Nevertheless, when narrowband signals are employed in the source distribution, a condition that is required due to the numerical errors that the FDTD method introduces at high frequencies and due to the assumption of frequency-independent impedances, the problem can become ill-posed leading to a worse convergence of the optimiza-

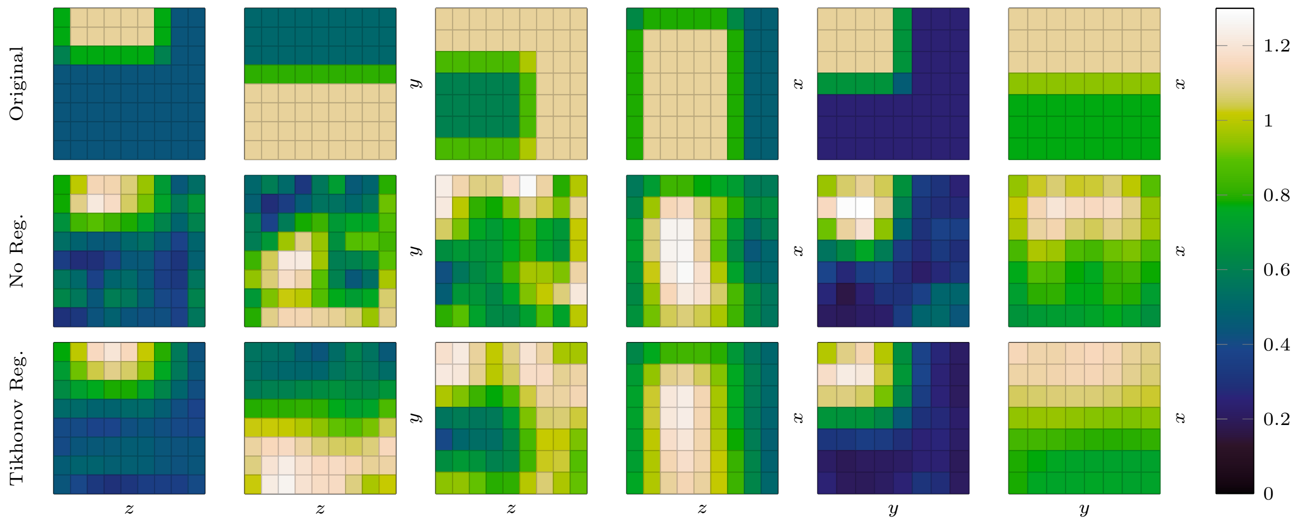

Figure 2. Surface admittances of the six faces of the cuboid room: left wall, right wall, rear wall, front wall, floor and ceiling. First row figures are the original surface admittances, second and third row is the estimated admittances for each wall using a narrowband signal as source without regularization and with Tikhonov regularization, respectively. All admittances are normalized by the maximum value of the original admittance for each wall.

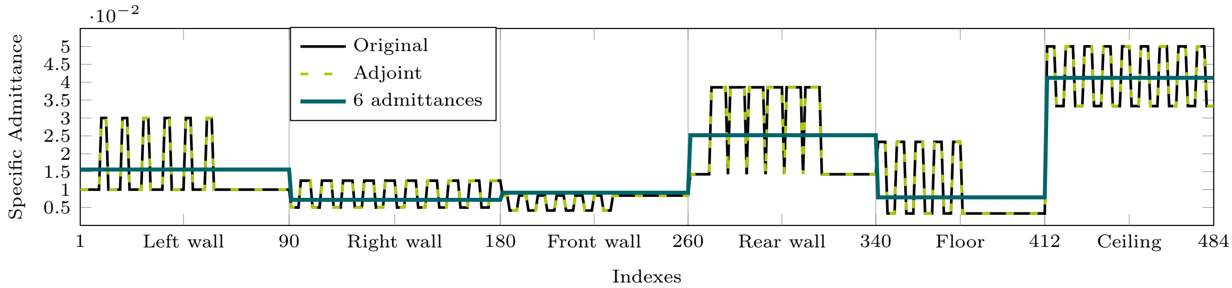

Figure 3. Plot of the original $\boldsymbol{v}$ vector and the estimated ones using the adjoint method and the GN method of [4] where only 6 admittances are used during the inversion procedure. The vertical lines divide the indexes corresponding to the different admittance surfaces. The original admittance values can also be viewed in 2D on the top row of Fig. 2.

tion method and reduced estimation accuracy. The usage of Tikhonov regularization can then help to obtain better results. Future work will focus on the usage of more effective regularizations and application of the method using real data.

Acknowledgement

This research work was carried out at the ESAT Laboratory of KU Leuven, in the frame of the FP7-PEOPLE Marie Curie Initial Training Network "Dereverberation and Reverberation of Audio, Music, and Speech (DREAMS)", KU Leuven Research Council CoE PFV/10/002 (OPTEC), the Interuniversity Attractive Poles Programme initiated by the Belgian Science Policy Office IUAP P7/19 "Dynamical systems control and optimization" (DYSCO) 2012-2017. The scientific responsibility is assumed by its authors.

References

[1] K. Kowalczyk and M. van Walstijn: Room acoustics simulation using 3-D compact explicit FDTD schemes. IEEE Trans. Audio, Speech Language Process., vol. 19, no. 1, pp. 34-46, Jan. 2011.

[2] F. Jacobsen, P. M. Juhl: Fundamentals of General Linear Acoustics, Wiley, 2013

[3] G. P. Nava, Y. Yasuda, Y. Sato, S. Sakamoto: On the in situ estimation of surface acoustic impedance in interiors of arbitrary shape by acoustical inverse methods. Acoust. Sci. & Tech., vol. 30, no. 2, pp. 100-109, Mar. 2009.

[4] N. Antonello, T. van Waterschoot, M. Moonen, P. Naylor: Identification of Surface Acoustic Impedances in a Reverberant Room Using the FDTD Method. Proc. 2014 Int. Workshop Acoustic Signal Enhancement (IWAENC 2014), Antibes, France, Sep. 2014.

[5] J. Virieux, S. Operto: An overview of full-waveform inversion in exploration geophysics. Geophysics 74, no. 6, WCC1-WCC26. Nov. 2009.

[6] D. A. Cook, M. F Mueller., F. Fedele, A.J. Yezzi: Adjoint Active Surfaces for Localization and Imaging, on IEEE Trans. Image Process. vol. 24, no. 1, pp. 316-331.

[7] J. Nocedal and S. J. Wright: Numerical Optimization, Springerverlang, 1999.

[8] P. C. Hansen, T. K. Jensen: Smoothing-norm preconditioning for regularizing minimum-residual methods. SIAM J. Matrix Anal. Appl., vol. 29, no. 1 pp. 1-14, Mar. 2006.